World Academy of Science, Engineering and Technology
International Journal of Electrical and Computer Engineering
Vol:13, No:2, 2019

Path-Tracking Controller for Tracked Mobile Robot on Rough Terrain

Toshifumi Hiramatsu, Satoshi Morita, Manuel Pencelli, Marta Niccolini, Matteo Ragaglia, Alfredo Argiolas

***Abstract*—**Automation technologies for agriculture field are needed to promote labor-saving. One of the most relevant problems in automated agriculture is represented by controlling the robot along a predetermined path in presence of rough terrain or incline ground. Unfortunately, disturbances originating from interaction with the ground, such as slipping, make it quite difficult to achieve the required accuracy. In general, it is required to move within 5-10 cm accuracy with respect to the predetermined path. Moreover, lateral velocity caused by gravity on the incline field also affects slipping. In this paper, a path-tracking controller for tracked mobile robots moving on rough terrains of incline field such as vineyard is presented. The controller is composed of a disturbance observer and an adaptive controller based on the kinematic model of the robot. The disturbance observer measures the difference between the measured and the reference yaw rate and linear velocity in order to estimate slip. Then, the adaptive controller adapts "virtual" parameter of the kinematics model: Instantaneous Centers of Rotation (ICRs). Finally, target angular velocity reference is computed according to the adapted parameter. This solution allows estimating the effects of slip without making the model too complex. Finally, the effectiveness of the proposed solution is tested in a simulation environment.

***Keywords*—**Agricultural robot, autonomous control, path-tracking control, tracked mobile robot.

I. Introduction

WITH rises in global population comes the problem of food shortages. For instance, in Japan the number of farmers is decreasing, while their average age is rapidly increasing. In the near future, this situation will likely result in shortages in food production [1]. Eventually, the same issue is expected to happen all over the world. For these reasons, automation technologies such as autonomous driving are needed to work large fields with fewer farmers. On the other hand, environmental problems such as soil structure damage have been identified due to the increasing size of agricultural machines, especially in northern Europe. To this regard, small-sized tracked machines could represent a promising solution since larger contact area and lower contact pressure between the tracks and the ground would ensure at the same time better motion performance and lower pressure on soil [2], [3]. Therefore, small-sized tracked mobile robots will likely spread in the agricultural market in the next few years.

One of the most relevant problems in automated agriculture is represented by controlling a machine along a predetermined path in presence of rough terrain or inclined ground. Furthermore, the presence of ridges requires agriculture vehicles to move within 5-10 cm accuracy with respect to the predetermined path. Unfortunately, the effect of gravity on inclined fields (such as vineyards) may generate slipping phenomena, thus making it quite difficult for the robot to achieve the required accuracy. Moreover, slipping depends on soil conditions, which in turn depend on geographical location, climate and other environmental factors, that cannot be modelled in a simple and accurate way. In the scientific literature, several studies tackling the problem of slip estimation have been proposed. For instance, an approach based on gyro sensors and encoders has been proposed in [4]. Unfortunately, the estimated slip ratio is not accurate enough for being used in real-world applications. Approaches based on Kalman filtering have also been proposed to estimate and/or compensate slip phenomena [5]-[8]. Alternative solutions, relying on both dynamic models and Kalman filtering, proved to be effective in estimating slipping or, alternatively, in identifying the resulting variation of the ICRs [6]. However, the main limitation of these approaches consists of limited robustness with respect to rapidly changing soil conditions or inclined fields. In order to address these shortcomings, techniques based on disturbance observation have been recently proposed [9], [10]. The disturbance observer (DOB) basically consists of an inner-loop controller, whose primary role is to compensate uncertainly in the plant and to reject exogenous process disturbances, thus making the inner-loop behave-like the nominal plant model.

The main contribution of this paper consists of the design of a control algorithm for tracked vehicles. This algorithm ensures path-tracking capabilities while moving in presence of slip phenomena that are due to either rough terrain and/or ground inclination. At first, slipping rejection is realized by using the DOB to adapt the target velocities (linear and angular) computed by the tracking controller. Unfortunately, this solution does not perform very well on inclined fields, since in these scenarios slipping is mainly due to the lateral velocity caused by gravity. Nevertheless, whenever the robot slips, its linear velocity and turning radius change. Virtually, this situation is equivalent to considering ICRs as time-varying parameters, rather than fixed quantities. Consequently, slip rejection can be achieved by integrating a parametric kinematic model of the robot inside the control algorithm, thus allowing to define virtual ICRs and to compensate slipping by adapting the virtual kinematic parameter. As a result, the main advantages of this approach consist in eliminating the need to: (i) either measure or estimate the dynamic parameters of the system; (ii) re-tune control gains whenever soil conditions change.

Toshifumi Hiramatsu, Satoshi Morita, Manuel Pencelli, Marta Niccolini, Matteo Ragaglia, and Alfredo Argiolas are with the YANMAR R&D Europe SRL, Viale Galileo 3/A, 50125 Firenze, Italy (phone: +39-055-5121694; fax: +39-055-5121693; e-mail: toshifumi_hiramatsu@yanmar.com).

The remainder of this paper is structured as follows: in Section II we introduce the kinematic model of the robot and we describe the proposed controller. Then, in Section III, simulation results are presented and a comparison between the proposed controller and a conventional Lyapunov-based control law is discussed. Finally, conclusions are summarized in Section IV.

II. Path-Tracking Control Algorithm

A. Kinematic Model of the Robot

Fig. 1 shows the kinematic model of the tracked robot, where:

- a is the vehicle's tread (i.e. the distance between the left track and the right one);
- θ is the robot orientation with respect to the Cartesian Frame x-y;
- v is the vehicle linear velocity;
- ω is the vehicle angular velocity;

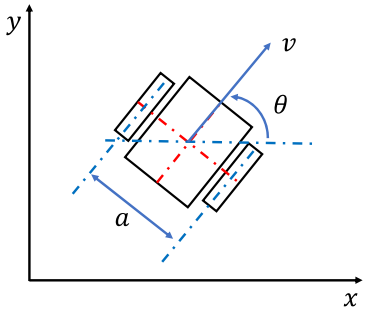

Fig. 1 Vehicle model

We consider a typical differential drive robot, whose kinematics can be modelled as follows [11]:

$$\begin{bmatrix}\dot{x}\\ \dot{y}\\ \dot{\theta}\end{bmatrix}=\begin{bmatrix}\cos\theta & 0\\ \sin\theta & 0\\ 0 & 1\end{bmatrix}\begin{bmatrix}v\\ \omega\end{bmatrix} \quad (1)$$

It is worth noticing that this kinematic model does not take into account slipping and skidding.

B. Path-Tracking Controller

The path-tracking problem is controlling linear and angular velocities such that the robot's trajectory follows a reference robot's trajectory as the reference path at a desired speed. The reference robot model is the following:

$$\begin{bmatrix}\dot{x}_r\\ \dot{y}_r\\ \dot{\theta}_r\end{bmatrix}=\begin{bmatrix}\cos\theta_r & 0\\ \sin\theta_r & 0\\ 0 & 1\end{bmatrix}\begin{bmatrix}v_r\\ \omega_r\end{bmatrix} \quad (2)$$

where v_r is the reference linear velocity, and ω_r is the reference angular velocity. We assume that v_r and ω_r, as well as their derivatives, are bounded. Moreover, we suppose that they do not tend to zero simultaneously. Given these hypothesis, we can define the equivalent trajectory tracking errors as:

$$\begin{bmatrix}e_1\\ e_2\\ e_3\end{bmatrix}=\begin{bmatrix}\cos\theta & \sin\theta & 0\\ -\sin\theta & \cos\theta & 0\\ 0 & 0 & 1\end{bmatrix}\begin{bmatrix}x_r-x\\ y_r-y\\ \theta_r-\theta\end{bmatrix} \quad (3)$$

According to [12], the following function

$$V_1=\frac{1}{2}(e_1^2+e_2^2)+\frac{1-\cos e_3}{K_2}. \quad (4)$$

is a valid Lyapunov function, provided that target velocities are set as follows:

$$\begin{aligned} v_d &= K_1 e_1 + v_r\cos e_3\\ \omega_d &= K_3\sin e_3 + K_2 e_2 v_r + \omega_r \end{aligned} \quad (5)$$

where K_1, K_2 and K_3 are control gains. Please notice that, at this stage, the control law ensures the convergence to zero of the errors, but it does not take into account slipping.

To compensate this phenomenon, we implement the DOB for both linear and angular velocity, as shown in Fig. 2. For the sake of clarity, the block labelled as "Path Tracking Control" refers to (5). We also consider the location of the ICRs as an unknown parameter that is estimated by the "Adaptive Control" block ($\widetilde{x_{ICR}}$) and sent as input to the Angular velocity DOB.

C. Disturbance Observer

Let us consider the side slipping due to lateral velocity caused by gravity on the incline field. According to [6], [13], we can re-write the robot kinematics model including the lateral velocity as:

$$\begin{bmatrix}\dot{x}\\ \dot{y}\\ \dot{\theta}\end{bmatrix}=\begin{bmatrix}\cos\theta & -\sin\theta & 0\\ \sin\theta & \cos\theta & 0\\ 0 & \frac{1}{x_{ICR}} & 1\end{bmatrix}\begin{bmatrix}v\\ v_y\\ \omega\end{bmatrix} \quad (6)$$

where v_y is lateral velocity, and x_{ICR} is the ICR location on the longitudinal direction. We assume that both v_y and its derivative are bounded and we define the nominal model of the Angular velocity DOB according to (6). Then, we consider the location of the ICR as an unknown parameter, thus using as input the virtual ICR location ($\widetilde{x_{ICR}}$) estimated by the adaptive controller. Finally, we define Q as the low-pass filter. As a result, we obtain the angular velocity DOB shown in Fig. 3.

Moving to the linear velocity, the nominal model is simply equal to "1", as it is shown Fig. 4. Given their structure, the two DOBs are able to compensate slip phenomena, thus guaranteeing that the system behaves as its nominal model [14].

D. Adaptive Control

In the previous section, we re-defined the angular velocity according to (6). Let us consider the Lyapunov function (4) again and let us compute the derivatives of (3), by substituting (5) and (6):

$$\begin{aligned} \dot{e_1} &= v_r\cos e_3 + e_2\dot{\theta} - v\\ \dot{e_2} &= v_r\sin e_3 - e_1\dot{\theta} - v_y\\ \dot{e_3} &= \omega_r - \omega - \frac{v_y}{x_{ICR}} \end{aligned} \quad (7)$$

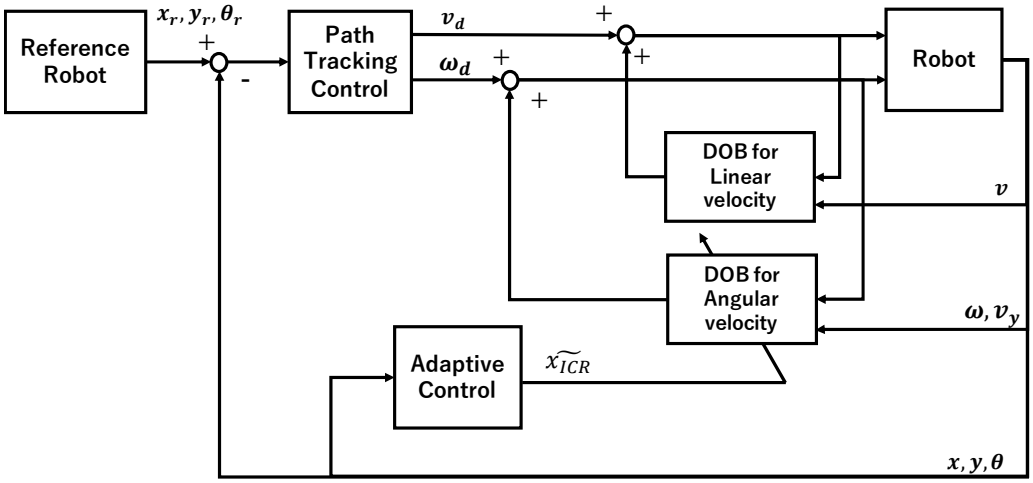

Fig. 2 Block diagram of controller

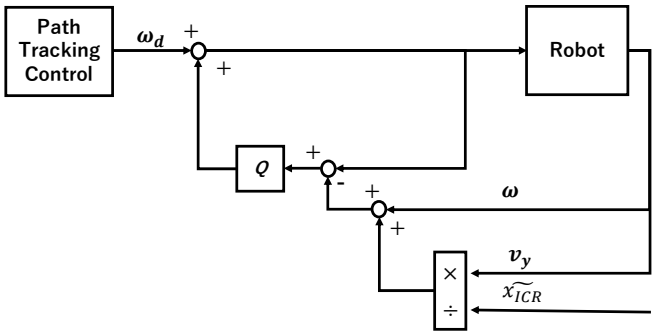

Fig. 3 Block diagram of Angular velocity DOB

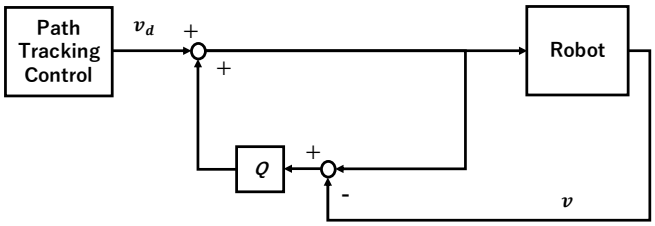

Fig. 4 Block diagram of linear velocity DOB

Then, the derivative of (4) can be computed as:

$$\dot{V}_1 = -e_1^2 K_1 - \frac{K_3}{K_2}(\sin e_3)^2 - (e_2 + \frac{\sin e_3}{K_2}\frac{1}{x_{ICR}})v_y \quad (8)$$

Now, let us introduce another Lyapunov candidate function, named V_2:

$$V_2 = V_1 + \frac{1}{2}y_d^2 \quad (9)$$

where y_d is the vehicle lateral displacement generated by v_y ($\dot{y}_d = v_y$). Since the tracked robot cannot move along this direction, y_d necessarily represents the lateral deviation caused by side slipping. By differentiating (9), we obtain:

$$\dot{V}_2 = \dot{V}_1 + y_d v_y \quad (10)$$

$$\dot{V}_2 = -e_1^2 K_1 - \frac{K_3}{K_2}(\sin e_3)^2 + (y_d - e_2 - \frac{\sin e_3}{K_2}\frac{1}{x_{ICR}})v_y. \quad (11)$$

If we define the estimate of the virtual ICR location $\widetilde{x_{ICR}}$ as:

$$\widetilde{x_{ICR}} = -\frac{1}{K_2}\frac{\sin e_3}{e_2 - K_4 v_y - y_d} \quad (12)$$

where K_4 is a positive control gain, we get:

$$\dot{V}_2 = -K_1 e_1^2 - \frac{K_3}{K_2}(\sin e_3)^2 - K_4 v_y^2 \leq 0. \quad (13)$$

Since V_2 is bounded from below and $\dot{V}_2$ is negative semi-definite, V_2 converge to a finite limit. As a consequence, e_1, e_2, e_3 and y_d are all bounded. Moreover, by considering (7) and (13), the second derivative of V_2 can be written as

$$\ddot{V}_2 = -2K_1 e_1 \left(v_r \cos e_3 + e_2\left(\omega_r - \frac{v_y}{x_{ICR}}\right) - v\right) - 2\frac{K_3}{K_2}\sin e_3 \cos e_3 \left(\omega_r - \omega - \frac{v_y}{x_{ICR}}\right) - 2K_4 v_y \dot{v}_y \quad (14)$$

From the above results, and since v_y and its derivative are bounded, we can state that also $\ddot{V}_2$ is bounded. Given the fact that: (i) V_2 is continuously differentiable respect to time, (ii) V_2 converges to some constant value, (iii) $\dot{V}_2$ is bounded, by Barbalat's lemma, $\dot{V}_2 \to 0$ as $t \to \infty$ [15], [16]. As a result, e_1, e_3 and v_y converge to zero. Moreover, the limit of the derivative of e_1 can be computed by combining (5) and (7), thus obtaining:

$$\lim_{t\to\infty} \dot{e}_1 = \lim_{t\to\infty} e_2(K_2 e_2 v_r + \omega_r) = 0. \quad (15)$$

Therefore, given a persistent reference signal ($\lim_{t\to\infty} v_r \neq 0$), either $e_2 \to 0$ or $e_2 \to -\omega_r / K_2 v_r$ as $t \to \infty$.

Let's assume at first that $e_2 \to -\omega_r / K_2 v_r$ as $t \to \infty$. In this case the derivative of e_1 and e_3 can be computed by combining once again (5) and (7):

$$\dot{e_1} \rightarrow -K_1 e_1 - \frac{1}{K_2}\frac{\omega_r}{v_r}\left(\frac{v_y}{x_{ICR}} + K_3 \sin e_3\right) \quad (16)$$

$$\dot{e_3} \rightarrow \omega_r - K_3 \sin e_3 - \frac{v_y}{x_{ICR}}. \quad (17)$$

As a consequence, $\dot{V}_2$ can be expressed in the following form:

$$\dot{V}_2 = -K_1 e_1^2 - \frac{K_3}{K_2}(\sin e_3)^2 - K_4 v_y^2 - \frac{\omega_r^2 v_y e_1}{K_2 v_r^2 \sin e_3} - \frac{K_4 \omega_r v_y^2 e_1}{v_r \sin e_3} - \frac{\omega_r v_y e_1 y_d}{v_r \sin e_3} - \frac{K_3 \omega_r e_1 \sin e_3}{K_2 v_r} + \frac{\omega_r \sin e_3}{K_2} - \frac{\omega_r v_y}{K_2 v_r}. \quad (18)$$

Equation (18) is not negative semi-definite. Since this result contradicts (13), in order to satisfy (15) it is necessary that $e_2 \rightarrow 0$ as $t \rightarrow \infty$.

III. Simulation Results

A. Simulation Model

The experimental platform used to test our controller is the Xbot, an electrically driven tracked mobile robot manufactured by Dronyx [17]. Fig. 5 shows the Xbot and its simulation model develop using V-Rep simulation environment [18]. Table I displays the main specification data of the Xbot.

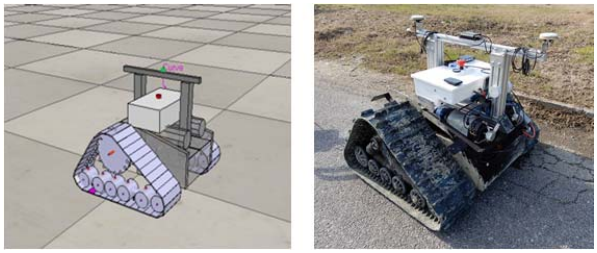

Fig. 5 Xbot in simulation and real field

TABLE I
Specification Data of Xbot

Specifications	Value
Weight	350 kg
Maximum payload,	200 kg
Maximum speed	2.5 km/h
Dimensions	1200 mm (length) 1200 mm (width)

In order to simulate the motion of the tracks, we use a wheel-based model, as shown in Fig. 6. The system contains 6 rollers per side that are in contact with the ground surface. The vehicle is able to move thanks to the friction force generated by each wheel. The friction force is computed by the Vortex physical engine developed by CM Labs [19]. Further details regarding the simulation models of the tracks can be found in [20].

B. Simulation Results

Moving to simulation results, Fig. 7 shows the comparison between the robot trajectory obtained in simulation and its counterpart experimentally measured on asphalt ground, proving that the proposed simulation model is accurate enough for our purpose. On the other hand, Fig. 8 shows an example of simulation inside a vineyard-like environment, where we set the incline angle to 10 degrees.

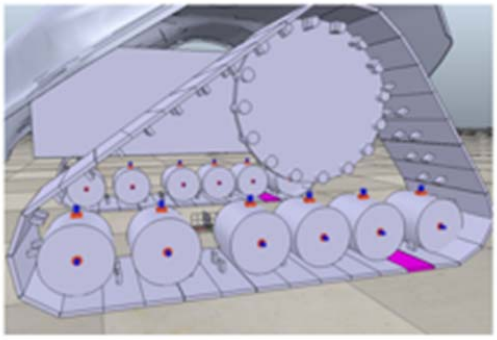

Fig. 6 Wheel-based track model

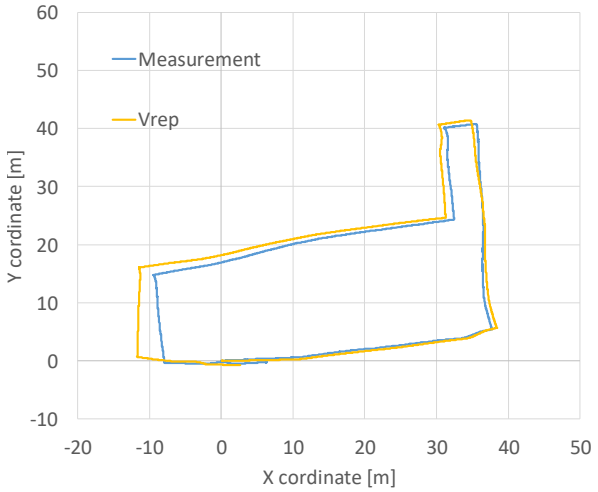

Fig. 7 Comparison of simulation and experimental results

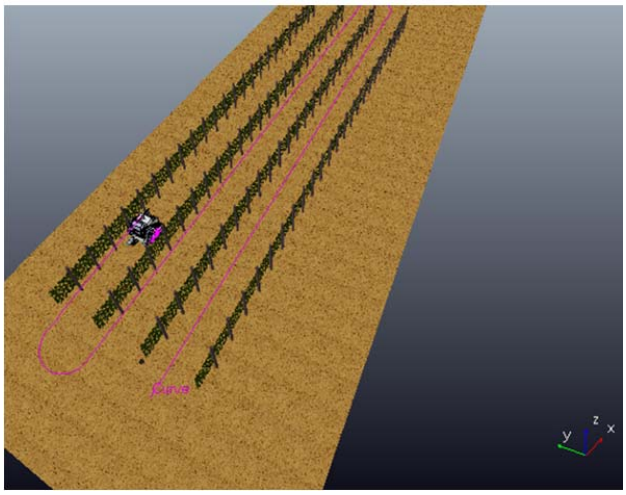

Fig. 8 Vineyard-like simulation environment

A first simulation is performed by making the robot climb along a straight reference path. In order to simulate slipping phenomena (due for instance to the presence of mud) we reduce the target speed of the right track by 20% in the interval

between 10 and 13 seconds from the simulation start. We refer to the Lyapunov-based control law (5) as "Conventional controller", while we refer to our proposed controller as "Adaptive DOB". We set the target speed as 0.5 m/s, and controller gains as $(K_1, K_2, K_3, K_4) = (1.2, 1.8, 2.0, 0.5)$ for both controllers. Finally, the cut off frequency of the low pass filter inside to DOB is set to 2 Hz. Fig. 9 shows how the two controllers are able to track the straight reference path, but it also demonstrates the superior performance of the Adaptive DOB in terms of reduce lateral deviation from the reference path.

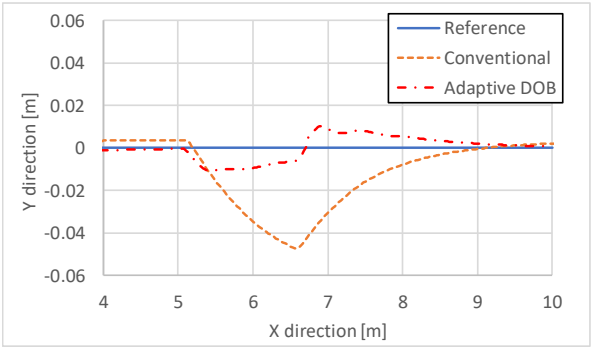

Fig. 9 Tracking trajectory result

More in depth, Fig. 10 shows the lateral error, i.e. the tracking error e_2 in (3). Before the robot starts slipping (i.e. prior to 10 sec) the two controllers entail similar performance. As soon as the robot starts slipping, the conventional controller is not able to reject the disturbance effectively and the lateral error significantly increases. On the other hand, the Adaptive DOB is able to reject the slipping and to limit the lateral error.

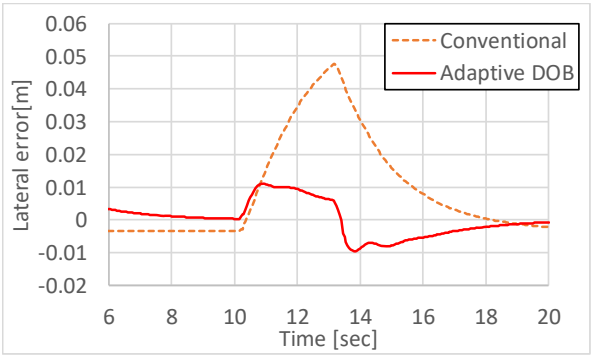

Fig. 10 Lateral error

Fig. 11 shows the results of different simulations during which the robot follows a typical vineyard-like trajectory. More in depth, the robot starts by climbing along the field, it performs a 180 degrees turn, it descends the field, it makes another 180 degrees turn, and, finally, it climbs along the field once again. The vehicle speed is 0.5 m/s, and the controllers are tuned with the previously displayed gains. Differently from the previous scenario, in this case a third control algorithm was considered in addition to the conventional controller and the adaptive DOB. This third controller is labelled as "Normal DOB" and it consists in a version of the DOB that relies only on kinematic model (1), without taking into account nor lateral velocity, neither adaptive parameters.

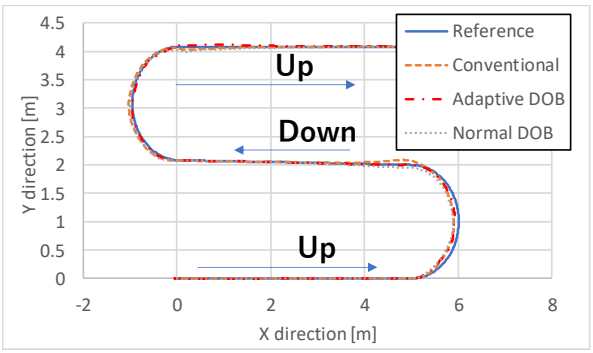

Fig. 11 Tracking trajectory results about second scenario

Fig. 12 demonstrates that the Adaptive DOB entails better performance in terms of reduced lateral error with respect to the conventional one. Moreover, the comparison between the adaptive DOB and the normal DOB shows that the convergence of the error to zero is much faster when considering the adaptive kinematic model, thus proving that the adaptive controller is able to better counteract the effect of the lateral velocity caused by gravity.

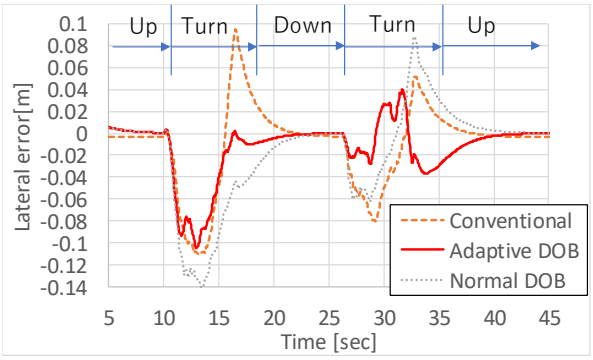

Fig. 12 Lateral error

We also compared the performance of the different control algorithms in terms of Root Mean Square Errors, as it is shown in Table II. As expected, the Adaptive DOB performs better than both the Conventional controller and the Normal DOB.

TABLE II
SIMULATION RESULTS (RMSE)

Error	Conventional controller	Adaptive DOB	Normal DOB
Lateral error	3.9 cm	2.9 cm	4.6 cm

Finally, Fig. 13 shows the results corresponding to a third simulation scenario, where the robot climbs the fields with a linear speed of 0.7 m/s before making a 270 degrees turn. Once again, Fig. 14 shows the lateral error. Not differently from the previous simulations, the adaptive DOB demonstrates superior performance in terms of reduced lateral error. As far as RMSE is concerned, Table III shows that the Adaptive DOB

guarantees a significantly lower error with respect to the conventional controller.

TABLE III
SIMULATION RESULTS (RMSE)

Error	Conventional controller	Adaptive DOB
Lateral error	4.6 cm	2.6 cm

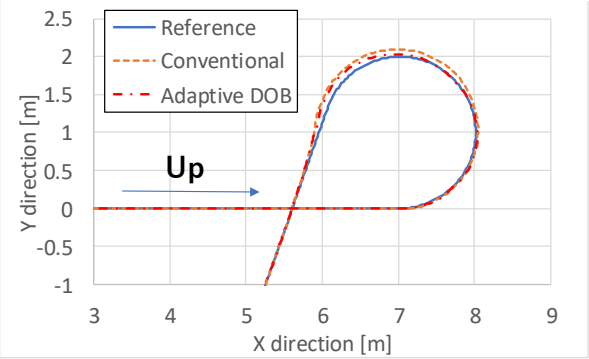

Fig. 13 Tracking trajectory about third scenario

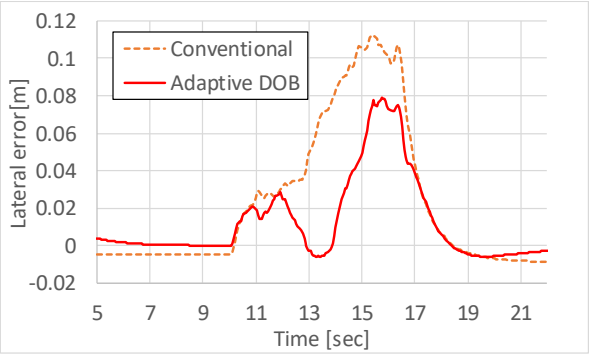

Fig. 14 Lateral error about third scenario

IV. CONCLUSION

In this paper, we propose a control algorithm for tracked vehicles that ensures path-tracking capabilities while moving in presence of slip phenomena, due to either rough terrain and/or ground inclination. The algorithm relies on the combination between a DOB and a parametric kinematic model in order to compensate slip phenomena. An adaptive control law allows to modify the parameter of the model in order to let the DOB robustly compensate slipping. The performance of the proposed controller is verified in simulation environment. A comparison between the proposed controller and a more conventional one is also discussed.

REFERENCES

[1] N. Noguchi and O. C. Barawid Jr., "Robot farming system using multiple robot tractors in Japan agriculture", In *18th IFAC world congress*, 2011.
[2] S. Blackmore, "New concepts in agricultural automation", In *HGCA conference*, 2009.
[3] D. Ball, P. Ross, A. English, P. Milani, D. Richards, A. Bate, B. Upcraft, G. Wyeth and P. Corke, "Farm workers of the future", In *IEEE Robotics & Automation magazine*, 2017.
[4] Y. Okada, D. Endo, K. Yoshida and K. Nagatani, "Trajectory control of crawler type mobile robot with consideration of a slip", In *The Robotics and Mechatronics Conference,* 2007.
[5] N. Shalal, T. Low, C. McCarthy and N. Hancock, "A review of autonomous navigation systems in agricultural environments", In *SEAg 2013*.
[6] J. Pentzer, S. Brennan and K. Reichard, "Model-based Prediction of Skid-steer Robot Kinematics Using Online Estimation of Track Instantaneous Centers of Rotation", In *Journal of Field Robotics*, 2014.
[7] R. Lenain, B. Thuilot, C. Cariou and P. Martinet, "Adaptive and predictive nonlinear control for sliding vehicle guidance", In *IEEE/RSJ International conference on Intelligence Robots and Systems,* 2014.
[8] H. Fang, R. Fan, B. Thuilot and P. Martinet, "Trajectory tracking control of farm vehicles in presence of sliding", In *IEEE/RSJ International conference on Intelligent Robots and Systems*, 2005.
[9] C. Wen-Hua, Y. Jun, G. Lei and L. Shihua, "Disturbance-observer-based control and related methods – An overview," In *IEEE Transl. Industrial electronics., vol. 63*, Feb. 2016, pp. 1083–1095
[10] S. Hyungbo, P. Gyunghoon, J. Youngjun, B. Juhoon and J. Nam Hoon, "Yet another tutorial of disturbance observer: robust stabilization and recovery of nominal performance", In *Control theory and technology. South China University of technology and academy of mathematics and systems science, vol. 14*, Aug., 2016, pp. 237-249
[11] R. Gonzàlez, R. Rodoriguez and J. Guzmàn, "Autonomous Tracked Robots in Planar Off-Road Conditions", Springer, 2014.
[12] Y. Kanayama, Y. Kimura, F. Miyazaki and T. Noguchi, "A Stable Tracking Control method for an autonomous mobile robot", In *Proceedings of IEEE International Conference on Robotics and Automation*, 1990.
[13] T. M. Dar and R. G. Longoria, "Estimating traction coefficients of friction for small-scale robotic tracked vehicles", In *Proceedings of the ASME 2010 Dynamics Systems and Control Conference*, 2010
[14] B. M. Nguyen, H. Fujimoto, Y. Hori, "Yaw angle control for autonomous vehicle using Kalman filter based disturbance observer", In *SAEJ. EVTeC and APE Japan,* 2014.
[15] J.-J. E. Slotine and W. Li, "Applied Nonlinear Control", Prentice Hall, 1991.
[16] F. Pourboghrat and M. P. Karlsson, "Adaptive control of dynamic mobile robots with nonholonomic constraints", In *Computers and Electrical Engineering 28,* 2002.
[17] Boost-up your research work without wasting time and money, retrieved January 25, 2019 from http://www.dronyx.com/xbot-tracked-mobile-robot/.
[18] V-rep virtual robot experimentation platform, retrieved January 25, 2019 from http://www.coppeliarobotics.com/.
[19] Achieve true-to-life simulation, retrieved January 25, 2019 from https://www.cm-labs.com/vortex-studio/features/physics-based-mechanical-dynamics-engine/.
[20] S. Morita, T. Hiramatsu, M. Niccolini, A. Argiolas, M. Ragaglia, "Kinematic track modelling for fast multiple body dynamics simulation of tracked vehicle robot", In *The 24th International Conference on Methods and Models in Automation and Robotics*, 2018.

Toshifumi Hiramatsu received Master of mechanical engineering degree from Kobe university (Japan) in 2010. He has been employed at YANMAR co., Ltd. since 2010. He is currently working as a robotics researcher at YANMAR R&D Europe.